

# Adaptive Cache Enhancement for Test-Time Adaptation of Vision-Language Models

Khanh-Binh Nguyen, Duc Thanh Nguyen  
Deakin University

Phuoc-Nguyen Bui, Hyunseung Choo  
Sungkyunkwan University

## Abstract

*Vision-language models (VLMs) demonstrate strong zero-shot generalization but degrade under distribution shifts in unlabeled downstream tasks. Test-Time Adaptation (TTA) enables online optimization during inference without annotations. Cache-based TTA methods maintain dynamic caches of low-entropy or high-confidence samples for efficient out-of-distribution adaptation. However, they encounter two key issues: (1) unreliable confidence metrics causing cache errors and reduced performance; and (2) inflexible decision boundaries failing to handle distributional variations. To address these, we propose the Adaptive Cache Enhancement (ACE) framework, which builds a robust cache by selectively storing high-confidence or low-entropy embeddings per class. It employs dynamic, class-specific thresholds initialized from zero-shot statistics and refined via exponential moving average and exploration-augmented updates, enabling adaptive class-wise boundaries for accurate predictions across diverse distributions. Experiments on 15 benchmarks show ACE achieves state-of-the-art results, outperforming existing TTA methods in challenging out-of-distribution scenarios.*

## 1. Introduction

Vision-language models (VLMs) such as CLIP [37] and ALIGN [19] exhibit remarkable zero-shot abilities in a wide range of tasks, including classification, retrieval, and segmentation [18, 20, 24, 49, 59, 63]. These models are trained to learn the semantic relationship between visual and textual information and can be used for image-text matching during inference. However, their effectiveness often decreases when handling unlabeled test data from domains that substantially differ from their training distribution [1, 30, 33].

To address the challenge of performance decline of VLMs to distribution shifts, test-time adaptation (TTA) has emerged as a strong and effective strategy for improving their adaptability in out-of-distribution (OOD) cases. Unlike supervised

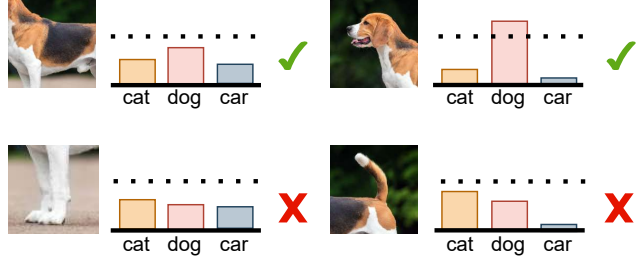


Figure 1. Noisy CLIP predictions on different views of a “dog”. CLIP can be overconfident on the simple views and fail on others.

fine-tuning or prompt learning, which requires expensive labeled data, TTA exploits unlabeled test data to dynamically adjust model predictions during inference. This characteristic makes TTA suitable for real-world applications, such as autonomous systems and medical imaging, where annotated datasets are often limited.

Prompt-based TTA methods [10, 13, 41] reduce the prediction entropy of VLMs by optimizing domain-specific prompts. However, their prompting optimization requires repeated backpropagation through the encoders of VLMs, resulting in substantial computational cost and hence limiting their scalability in resource-limited settings. Cache-based TTA strategies [21, 52, 55, 56] dynamically assemble a cache of high-confidence samples guided by VLM prediction entropy metrics, thus fine-tuning predictions with minimal parameter changes. For example, TDA [21] uses adaptive caching to enhance the calibration of predictions, while DMN [56] utilizes short- and long-term memory banks to leverage past insights. Similarly, DPE [52] improves multimodal alignment through dual-modal residual learning.

However, as demonstrated in Figure 1, CLIP predictions vary significantly under different augmentations, making the entropy-based sample selection unreliable and potentially hindering the adaptability of the model [7, 23]. Furthermore, the decision boundaries of the VLMs in target domains become inconsistent. Even with TTA, these models frequently fail to adjust the decision boundaries to accommodate domain shifts, resulting in fluctuating predictions. Although

several methods [52, 56] attempt to overcome this issue by using mean textual prototypes from enriched prompts, they are limited in handling the variability from intra-class diversity shifts.

To address the above challenges, we propose the Adaptive Cache Enhancement (ACE) framework, which constructs a robust cache by selectively storing high-confidence or low-entropy image embeddings for each class, directed by dynamic, class-specific thresholds initialized from zero-shot statistics and iteratively refined with an exponential moving average and exploration-augmented updates. By excluding overconfident samples from the cache, our method avoids overfitting, allows for adaptable class-specific decision boundaries, and ensures reliable and precise predictions across a broad range of data distributions. To this end, we make the following contributions in our work.

- We propose ACE, a novel framework for boosting up the performance of VLMs in domain shifts.
- We introduce an adaptive and class-wise thresholding mechanism to enhance the reliability of predictions across diverse data distributions. Our thresholding mechanism is initialized from zero-shot statistics and refined via exponential moving average and exploration-augmented updates.
- We validate the robustness and generality of our method through extensive experiments on 15 benchmark datasets and show the superiority of our ACE over current research in challenging OOD scenarios.

## 2. Related Work

### 2.1. Vision-Language Models (VLMs)

Large-scale pre-trained VLMs such as CLIP [37] have demonstrated substantial proficiency in acquiring transferable representations that span both imagery and text. Extensive research has been conducted to optimize these models for downstream applications. Initial efforts, including prompt learning strategies [59, 60], achieve notable success by implementing minimal supervision in few-shot learning environments. Recent methods, e.g., Tip-Adapter [53] and TaskRes [50], have effectively utilized feature memories derived from a limited number of labeled instances for rapid adaptation. These memory-based approaches have gained popularity due to their ability to facilitate quick domain adaptation with minimal computational burden, eliminating the requirement for full model fine-tuning. Nevertheless, their dependency on labeled target-domain data limits their applicability in real-world contexts, where such data are often not available. Our research focuses on test-time adaptation, which compels VLMs to acclimate to new domains during the inference stage without access to labeled data. This scenario closely reflects the real-world setting, advancing the development of flexible vision-language systems.

### 2.2. Test-Time Adaptation (TTA) for VMLs

Test-time adaptation (TTA) improves vision-language models (VLMs) adaptability to unfamiliar domains using only unlabeled test data [7, 27, 41, 58]. Methods fall into prompt-based and cache-based categories. Prompt-based approaches refine textual embeddings during inference, such as TPT [41] for augmented view consistency and DiffTPT [10] for diffusion-augmented diversity. In contrast, cache-based methods leverage historical test samples, including TDA [21] for positive/negative feature caches, DMN [56] for static/dynamic memory integration, and DPE [52] for parallel prototype refinement. While prompt-based methods are simple, cache-based ones offer better adaptability and efficiency via lightweight domain modeling. Recent advances include BCA [62] (Bayesian priors with overhead), FreeTTA [5] (training-free online EM/GMM), COSMIC [17] (semantic cliques), and AWT [64] (augmentation-weighting-transport), yet they neglect class-specific threshold dynamics under shifts. Building on cache-based techniques, our work enhances cache quality through reliable selection and predictive strength via adaptive decision boundaries; ACE distinctively employs EMA-refined thresholding to boost reliability and intra-class diversity handling.

Method	Key Mechanism	Adaptive Thresholds	Class Specific	Efficiency Focus
BCA	Bayesian priors	No	Partial	No
FreeTTA	Online EM/GMM	No	No	Yes*
COSMIC	Semantic cliques	No	No	Yes
AWT	Augment/Weight/Transport	No	No	Partial
ACE (Ours)	Curriculum + Exploration Thresholding	Yes	Yes	Yes

Table 1. Methodology comparison. '\*' denotes training-free.

## 3. Proposed Method

We propose an effective and reliable TTA strategy that includes a cache data structure, prototype residual learning modules, a flexible class-wise thresholding mechanism, and an adaptive threshold refinement module based on the statistic of pseudo-labels. We realize our method with CLIP [37], a state-of-the-art VLM model, and DPE [52], a prototype residual vector learning technique.

### 3.1. Preliminaries

#### 3.1.1. Zero-shot CLIP Prediction.

CLIP is pre-trained on a large collection of image-text pairs to align visual and textual information within an embedding space. CLIP can be trained by optimizing a contrastive loss that maximizes the cosine similarity between matching image-text pairs. CLIP comprises a visual encoder  $\mathcal{E}_v$  and a text encoder  $\mathcal{E}_t$ , which map images and text into a shared latent space  $\mathbb{R}^d$ . At inference time, an image  $x$  is classified

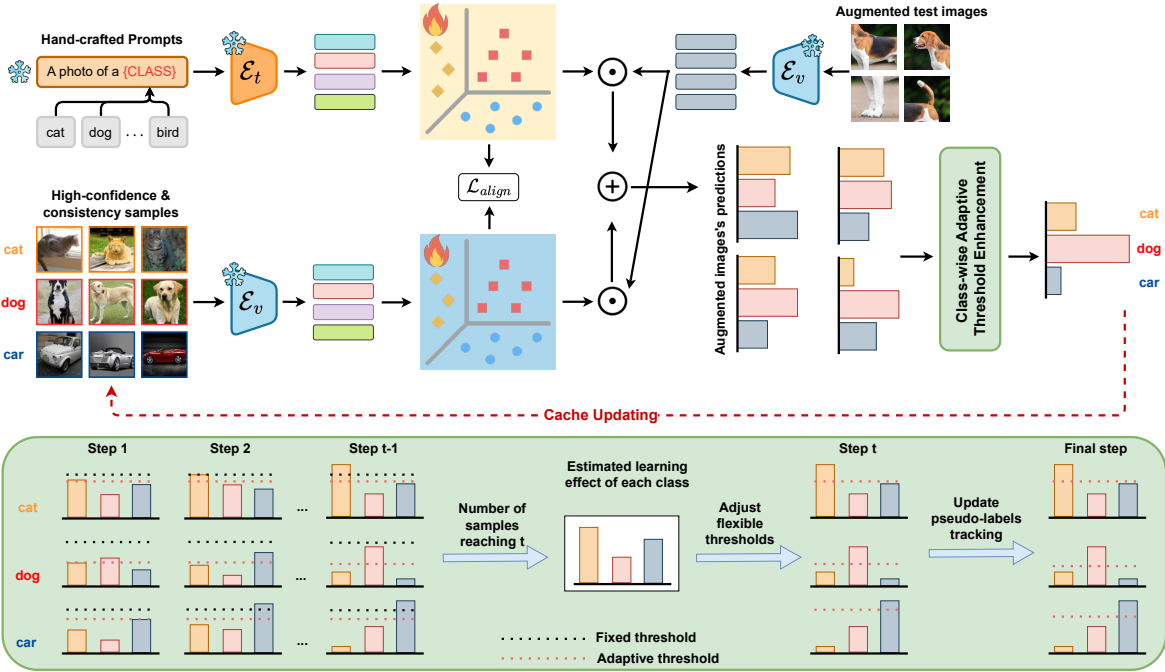


Figure 2. **Overview of the ACE Method.** We introduce the Class-wise Adaptive Threshold Enhancement module, which refines the threshold online to allow more correct samples but low-confidence samples to be cached. By simultaneously minimizing entropy loss for the prototype residuals and creating highly reliable caches, ACE enhances the overall multimodal generalization and robustness.

by measuring the similarity between its visual representation  $\mathbf{z} = \mathcal{E}_v(x)$  and textual embeddings  $\mathbf{t}^c = \mathcal{E}_t(\mathcal{P}^c)$ , where  $\mathcal{P}^c$  is a text prompt describing a class  $c$ , and  $C$  is the total number of classes. The zero-shot CLIP prediction probability is then given by:

$$p_{\text{CLIP}}^c = \frac{\exp(\mathbf{z} \cdot \mathbf{t}^c / \tau)}{\sum_{j=1}^C \exp(\mathbf{z} \cdot \mathbf{t}^j / \tau)} \quad (1)$$

where  $\tau$  is the temperature parameter, typically set to 0.01.

### 3.1.2. Cache-based TTA.

Inspired by the key-value storage framework introduced in TIP-Adapter [54], several cache-based TTA approaches [21, 52, 55] have been proposed, which dynamically store and update high-confidence feature-label pairs during inference. The cache is organized as a priority queue, where the priority of each entry is determined by the entropy of CLIP's predictions.

Let  $\mathbf{W}_{\text{CLIP}} = [\mathbf{t}^1, \mathbf{t}^2, \dots, \mathbf{t}^C]^\top$  be a stack of text embeddings for all classes. Cache item is represented as:

$$\{\mathbf{F}_{\text{cache}}, \mathbf{L}_p, \mathcal{H}(\mathbf{F}_{\text{cache}} \mathbf{W}_{\text{CLIP}}^\top)\}, \quad (2)$$

where  $\mathbf{F}_{\text{cache}}$  denotes the stored image features,  $\mathbf{L}_p$  is a one-hot pseudo-label predicted by CLIP, and  $\mathcal{H}(p)$  is the entropy:

$$\mathcal{H}(p) = \left( - \sum_{i=1}^C p_i \log p_i \right) \quad (3)$$

As test samples arrive sequentially, new entries are inserted into cache slots corresponding to their pseudo-labels. When the cache exceeds its capacity, the entries with the highest entropy are evicted. During inference, a test feature  $\mathbf{z}$  retrieves related cache items, and the final prediction is calculated by combining the CLIP logits with those derived from the cache:

$$\text{logits}_{\text{cls}}(\mathbf{z}) = \mathbf{z} \mathbf{W}_{\text{CLIP}}^\top + \mathcal{F}(\mathbf{z} \mathbf{F}_{\text{cache}}^\top) \mathbf{L}_p, \quad (4)$$

where  $\mathcal{F}(x) = \alpha \exp(-\beta(1 - x))$  is a modulation function with a scaling factor  $\alpha$  and a sharpness parameter  $\beta$ .

Following the DPE approach Zhang et al. [52], the feature for each cache slot,  $\mathbf{F}_{\text{cache}}$ , is computed as the mean of all stored features for that class, forming increasingly compact and representative class-specific prototypes as more data accumulates. The cache item is then constructed as:

$$\{\mathbf{F}_{\text{cache}}, \mathbf{L}_p, \mathcal{H}(\mathbf{F}_{\text{cache}} \mathbf{W}_{\text{CLIP}}^\top) \leq \mathcal{T}\}, \quad (5)$$

where  $\mathcal{T}$  is an entropy threshold for the caching decision.

### 3.2. Adaptive Cache Enhancement (ACE)

Cache-based strategies demonstrate notable effectiveness in various domains. However, they are grappling with two substantial issues. First, entropy is not a reliable indicator when the data distribution changes. Second, fixed decision boundaries are not adaptive to distributional changes. To

address these challenges, we introduce two specialized modules that specifically address each issue while synergistically strengthening each other, as illustrated in Figure 2. In our framework, we explore two variants of ACE to accommodate different confidence estimation strategies: ACE-Entropy and ACE-Probability. ACE-Entropy employs entropy  $\mathcal{H}(p)$  as the primary metric for cache selection and threshold refinement. In contrast, ACE-Probability uses maximum class probability  $\max(p_c)$  for thresholding. Both are initialized from zero-shot statistics and updated via EMA, and both maintain computational parity, with no additional overhead.

### 3.2.1. Curriculum Thresholding

The task of dynamically setting class-specific thresholds in alignment with the evolving learning progress of the model is challenging. Ideally, the threshold for each class can be set specifically based on evaluation metrics, e.g., recognition accuracy or entropy as  $\mathcal{T}_t(c) = m_t(c) \cdot \mathcal{T}_0(c)$ , where  $\mathcal{T}_t(c)$  is the adaptive threshold for class  $c$  at time step  $t$ , and  $m_t(c)$  denotes the corresponding metric, whether it is accuracy or entropy. This ensures that classes with poorer performance, indicated by lower accuracy rates, are designated smaller thresholds (or conversely, higher entropy leads to larger thresholds), thereby permitting a greater number of their instances to be retained in the cache during the testing phase. However, dynamically adjusting these thresholds throughout the training process requires continuous accuracy estimates at time increments  $t$ , which impedes training efficiency.

In this study, we introduce Curriculum Thresholding, a thresholding mechanism that evaluates the learning status of classes without introducing any additional inference steps and/or requiring additional annotations. Central to our hypothesis is the postulation that when subjected to a high threshold, the quantity of confidently classified predictions ascribed to a particular class serves as a robust indicator of the learning progress for that class. Specifically, we proceed with the following steps:

$$\begin{aligned}\sigma_t(c) &= \sum_{n=1}^N \mathbb{1}(\max(p(y|x)) \geq \mathcal{T}_{t-1}(c)) \cdot L_p^c, \\ \text{or} &= \sum_{n=1}^N \mathbb{1}(\min(e(y|x)) \leq \mathcal{T}_{t-1}(c)) \cdot L_p^c, \\ L_p^c &= \begin{cases} 1, & \text{if } \arg \max(p(y|x)) = c \\ 0, & \text{otherwise} \end{cases}\end{aligned}$$

where  $\sigma_t(c)$  measures the number of samples confidently predicted as class  $c$  at time  $t$ , and  $p(y|x)$  and  $e(y|x)$  are the probability and entropy of the model to sample  $x$ . We then normalize  $\sigma_t(c)$  as  $\sigma_t(c) \leftarrow \frac{\sigma_t(c)}{\max_c \sigma_t}$

Intuitively, a higher  $\sigma_t(c)$  indicates that the model has learned class  $c$  more effectively. Next, we compute an adaptive threshold  $\mathcal{T}_t(c)$  for class  $c$  at time step  $t$  using the Exponential Moving Average (EMA) as,

$$\mathcal{T}_t(c) = \delta \mathcal{T}_{t-1}(c) + (1 - \delta) \cdot m_t(c) \quad (6)$$

where  $m_t(c) = \sigma_t(c) \cdot m_{t-1}(c)$  is the latest performance metric (accuracy or entropy) and  $\delta$  is an EMA factor.

Nevertheless, considering that Eq. (6) is executed solely during the testing phase, it should be anticipated that initial performance might not be optimal. To improve the adaptability and reduce overfitting of the model, particularly for classes well-represented in the dataset, the initial threshold at time  $t = 0$  is determined using statistics from zero-shot learning. This statistic is simply the average of the entropy and probability across all samples in the test set. This initialization effectively captures the true behavior of both the model and the test set, ensuring reliable and meaningful results. It is important to highlight that incorporating CT is essentially cost-effective. In practice, whenever the confidence level of a sample's prediction surpasses the threshold  $\mathcal{T}$ , the sample, along with its predicted class, is flagged. Flagged instances will be retained in the cache in subsequent iterations.

### 3.2.2. Online Thresholding Adaptation

The CLIP model exhibits limitations in terms of its applicability across all datasets. Consequently, in scenarios such as zero-shot evaluations or even during TTA, predictions may not always be made for certain classes. It is critical to monitor classes that have been encountered infrequently or not at all. For these infrequently seen or never-seen classes, we implement a strategy for more intensive threshold exploration. This approach enhances the diversity of the cache and accelerates the adaptation to classes that exhibit a long-tailed distribution. To streamline our analysis, we categorize any class with fewer than 10 predictions as rarely seen classes.

$$\begin{aligned}\text{Never seen : } \mathcal{T}_t(c) &= \sum_1^C \mathbb{1}(M_{c,t} = 0) * \mathcal{T}_t(c) * (1 - \gamma) \\ \text{Rarely seen : } \mathcal{T}_t(c) &= \sum_1^C \mathbb{1}(M_{c,t} \leq 10) * \mathcal{T}_t(c) * (1 - \gamma * 0.5)\end{aligned}$$

where  $\gamma$  is an adaptation rate and  $M_{c,t}$  is the number of samples of class  $c$  at time  $t$  in the cache.

The online thresholding adaption ensures that the best-learned class reaches the full threshold  $\mathcal{T}$ , while the less-learned classes get proportionally lower thresholds, encouraging more of their samples to be trained. As the training progresses, the model improves and the thresholds converge towards  $\mathcal{T}$ . Notably, the thresholds are not guaranteed to increase over time; they may decrease if predictions become less confident in later iterations.

### 3.2.3. Test-Time Logit Inference and Loss Function.

We adopt DPE, the residual learning method proposed by Zhang et al. [57], to define textual and visual embedding

Method	ImageNet	ImageNet-A	ImageNet-V2	ImageNet-R	ImageNet-S	Average	OOD Average
CLIP-ResNet-50 [38]	58.16	21.83	51.41	56.15	33.37	44.18	40.69
Ensemble	59.81	23.24	52.91	60.72	35.48	46.43	43.09
CoOp [61]	63.33	23.06	55.40	56.60	34.67	46.61	42.43
TPT [40]	60.74	26.67	54.70	59.11	35.09	47.26	43.89
DiffTPT [11]	60.80	31.06	55.80	58.80	37.10	48.71	45.69
TDA [22]	61.35	30.29	55.54	62.58	38.12	49.58	46.63
TPS [44]	61.47	30.48	54.96	62.87	37.14	49.38	46.36
DMN-ZS [57]	63.87	28.57	56.12	61.44	39.84	49.97	46.49
DPE [52]	63.41	30.15	56.72	63.72	40.03	50.81	47.66
CRG [51]	<b>65.26</b>	29.69	56.07	-	-	-	-
<b>ACE-Probability</b>	<u>64.41</u>	<u>33.50</u>	<u>57.50</u>	<b>63.95</b>	<u>40.15</u>	<u>51.75</u>	<u>49.37</u>
<b>ACE-Entropy</b>	64.30	<b>33.55</b>	<b>57.51</b>	<u>63.82</u>	<b>40.25</b>	<b>51.78</b>	<b>49.38</b>
CLIP-ViT-B/16 [38]	66.73	47.87	60.86	73.98	46.09	59.11	57.20
Ensemble	68.34	49.89	61.88	77.65	48.24	61.20	59.42
CoOp [61]	71.51	49.71	64.20	75.21	47.99	61.72	59.28
TPT [40]	68.98	54.77	63.45	77.06	47.94	62.44	60.81
DiffTPT [11]	70.30	55.68	65.10	75.00	46.80	62.28	60.52
TDA [22]	69.51	60.11	64.67	80.24	50.54	65.01	63.89
TPS [44]	70.19	60.08	64.73	80.27	49.95	65.04	63.76
DMN-ZS [57]	72.25	58.28	65.17	78.55	<b>53.20</b>	65.49	63.80
DPE [52]	71.91	59.63	65.44	80.40	52.26	65.93	64.43
CRG [51]	<b>75.01</b>	<b>63.67</b>	64.66	-	-	-	-
<b>ACE-Probability</b>	72.56	<u>63.54</u>	<u>65.86</u>	<u>81.01</u>	52.60	<u>67.05</u>	<u>66.01</u>
<b>ACE-Entropy</b>	<u>72.57</u>	63.47	<b>65.91</b>	<b>81.09</b>	<u>52.66</u>	<b>67.10</b>	<b>66.05</b>

Table 2. Performance comparisons on robustness to natural distribution shifts. We present top-1 accuracy (%) results for all evaluated methods employing both ResNet-50 and ViT-B/16 visual backbones of CLIP. The best and second-best results are highlighted in **bold** and underlined, respectively.

prototypes as  $\mathbf{t}_c = \frac{1}{S} \sum_{i=1}^S \mathcal{E}_t(\mathcal{P}_i^c)$  and  $\mathbf{v}_c = \frac{1}{S_c} \sum_{m=1}^{S_c} \mathbf{z}_m^c$ . Here,  $S$  is the number of prompts,  $S_c \leq M$  is the total count of image features stored in the queue corresponding to class  $c$ , and  $\mathbf{z}$  is the image features of  $x$  that surpass the threshold  $\mathcal{T}$ . Once the two sets of multi-modal prototypes have been adjusted based on the last test sample, they are used to serve as the initial configuration for further refinement with the current test input. The preliminary outcomes derived from these steps are subsequently utilized to fine-tune the prototypes, making them adapted to  $x$  as,

$$\mathbf{t}_c \leftarrow \frac{\mathbf{t}_c + \hat{\mathbf{t}}_c}{\|\mathbf{t}_c + \hat{\mathbf{t}}_c\|}, \quad \mathbf{v}_c \leftarrow \frac{\mathbf{v}_c + \hat{\mathbf{v}}_c}{\|\mathbf{v}_c + \hat{\mathbf{v}}_c\|}. \quad (7)$$

where  $\hat{\mathbf{t}}_c \in \mathbb{R}^{C \times d}$  and  $\hat{\mathbf{v}}_c \in \mathbb{R}^{C \times d}$  are the learnable residual parameters that are initialized as zero and are used to optimize the prototypes for each given test input  $x$ . Similarly to Zhang et al. [57], we optimize these residual parameters to

promote consistent predictions in a total of  $N$  different augmented views of each given test image  $x$  using the objective of unsupervised entropy minimization,

$$\begin{aligned} \mathcal{L}_{\text{aug}} &= \mathcal{H}(\mathbb{P}_{\text{ACE}}(x)) \\ &= - \sum_{c=1}^C \mathbb{P}_{\text{ACE}}(y = y_c|x) \log \mathbb{P}_{\text{ACE}}(y = y_c|x) \end{aligned} \quad (8)$$

where

$$\begin{aligned} \mathbb{P}_{\text{ACE}}(x) &= \frac{1}{\rho N} \sum_{n=1}^N \mathbb{1}[\mathcal{H}(\mathbb{P}_{\text{Proto}}(\mathcal{A}_n(x)) \leq \mathcal{T}_e) \mathbb{P}_{\text{Proto}}(\mathcal{A}_n(x))] \\ \text{or} &= \frac{1}{\rho N} \sum_{n=1}^N \mathbb{1}[p(\mathbb{P}_{\text{Proto}}(\mathcal{A}_n(x)) \geq \mathcal{T}_p) \mathbb{P}_{\text{Proto}}(\mathcal{A}_n(x))] \end{aligned}$$

where  $\mathcal{A}_n(x)$  is an augmented view of  $x$ ,  $\mathcal{T}_e$  and  $\mathcal{T}_p$  are the entropy threshold and probability threshold, respectively.

We adopt the alignment loss in DPE:

$$\mathcal{L}_{\text{align}} = \frac{1}{C} \sum_{c=1}^C -\log \left( \frac{\exp(\mathbf{t}_c^\top \mathbf{v}_c)}{\sum_{c'} \exp(\mathbf{t}_c^\top \mathbf{v}_{c'})} \frac{\exp(\mathbf{t}_{c'}^\top \mathbf{v}_c)}{\sum_{c'} \exp(\mathbf{t}_{c'}^\top \mathbf{v}_{c'})} \right) \quad (9)$$

The final objective for optimizing the multi-modal prototypes  $\mathbf{t}, \mathbf{v}$  is defined as,

$$\hat{\mathbf{t}}, \hat{\mathbf{v}} = \arg \min_{\mathbf{t}, \mathbf{v}} \{ \mathcal{L}_{\text{aug}} + \lambda \mathcal{L}_{\text{align}} \}, \quad (10)$$

After optimizing the prototypes for each test sample  $x$ , we evolve the online textual prototypes  $\mathbf{t}$ , and update the priority queues to re-compute the visual prototypes  $\mathbf{v}$ . Then, we perform the testing as usual as in Eq. (4).

## 4. Experiments

In this section, we assess the robustness of the proposed ACE method to natural distribution shifts and its cross-dataset generalization across 15 different datasets. In addition, we compare the test-time efficiency of ACE against existing approaches. Lastly, we conduct ablation studies to examine the impact of various components and design choices.

### 4.1. Experimental Setup

**Datasets** Following prior research [21, 52], we evaluate our method in two main benchmarking scenarios: cross-dataset generalization and robustness to natural distribution shifts. (1) For the cross-dataset generalization scenario, we carry out evaluations across 10 varied recognition datasets, including FGVC Aircraft [28], Caltech101 [8], Stanford Cars [25], DTD [3], EuroSAT [14], Flowers102 [32], Food101 [2], Oxford Pets [34], SUN397 [47], and UCF101 [42]. These datasets collectively offer a comprehensive benchmark to assess the adaptability and generality of models across different datasets. (2) To evaluate the robustness of our method against natural distribution shifts, we test our method with ImageNet [6] and its out-of-distribution variants, including ImageNet-A [16] and ImageNet-V2 [39]. This part of the evaluation assesses our method’s robustness under varying distribution shifts. For datasets with particularly large test sets, e.g., Food101, ImageNet, SUN397, ImageNet-V2, and ImageNet-A, we sample 2,000 test instances for evaluation, adhering to the experimental protocol in DiffTPT [12].

**Implementation details** Following previous studies [21, 52], we select ResNet-50 and ViT-B/16 as visual encoders for CLIP, employing hand-crafted prompts as described in the supplementary material. In line with the method by [41], we create 63 augmented views per test image. The AdamW optimizer is used with the learning rate set to 0.0005 for the residual parameters in one iteration. Hyperparameters are set as follows:  $\alpha = 6$ ,  $\beta = 5.0$ ,  $\delta = 0.95$ ,  $\gamma = 0.02$ ,  $\lambda = 0.5$ ,

and queue size  $M = 16$  (since ACE shows resilience to noisy pseudo-labels and benefits from additional samples for class distribution modeling). All experiments are conducted on a single NVIDIA A100 GPU with 40GB of memory.

## 4.2. Results

**Robustness to Natural Distribution Shifts.** Our method reliably excels in adapting to varied image datasets with natural shifts, as highlighted in Table 2. Compared to TDA [21] and DPE [57], both our probability and entropy variants outperform them across 4 out of 5 datasets with notable differences, tested across ResNet-50 and ViT-B/16 backbones. Specifically, our ACE achieves top OOD average accuracies of 49.38% with ResNet-50 and 66.05% with ViT-B/16. While CRG [51] occasionally surpasses our method, we found this is due to the limited use of data augmentation in our experiments. Our method also outperforms the few-shot learning technique CoOp [59], underscoring our method’s robust ability to adapt VLMs to OOD scenarios.

**Cross-Datasets Generalization.** In Table 3, we evaluate the generality of our ACE-Probability and ACE-Entropy variants across 10 diverse fine-grained datasets, and compare them with state-of-the-art approaches. Due to significant distributional differences among these datasets, performance varies considerably. However, our methods achieve average accuracy improvements of 1.65% and 0.82% over the best-performing methods on the CLIP-ResNet-50 and ViT-B/16 backbones, respectively, surpassing competitors in 6 out of 10 datasets. Notably, on the challenging DTD dataset, characterized by complex texture categories, our approach consistently outperforms prior works across both CLIP backbones by a large margin. Additionally, our approach significantly outperforms the few-shot prompt learning method CoOp [59] in all datasets. These findings highlight the generality and adaptability of our approach in test-time domain transfer, making it highly suitable for real-world applications.

### 4.3. Ablation study

#### 4.3.1. Cache size and zero-shot statistics.

Table 4 presents an ablation study on the impact of zero-shot cache initialization and cache size on the performance of our ACE across five datasets. Table 4 (a) compares DPE with our ACE in two settings: with and without zero-shot (ZS) cache. As shown in the results, ACE with ZS cache achieves higher average accuracies (95.33% on Caltech and 77.30% on Flower with ViT-B/16) compared to DPE, highlighting the benefit of ZS cache initialization. Table 4 (b) examines the effect of cache size ( $M$ ) using probabilistic (Prob.) and entropy (Ent.) quantities. The results show that larger cache sizes (e.g.,  $M = 16$ ) consistently improve the classification performance of CLIP (95.33% on Caltech and 73.72% on UCF with ViT-B/16). These achievements highlight ACE’s

Method	Aircraft	Caltech	Cars	DTD	EuroSAT	Flower	Food101	Pets	SUN397	UCF101	Average
CLIP-ResNet-50	15.66	85.88	55.70	40.37	23.69	61.75	73.97	83.57	58.80	58.84	55.82
CoOp [59]	15.12	86.53	55.32	37.29	26.20	61.55	75.59	87.00	58.15	59.05	56.18
TPT [41]	17.58	87.02	58.46	40.84	28.33	62.69	74.88	84.49	61.46	60.82	57.66
DiffTPT [12]	17.60	86.89	<b>60.71</b>	40.72	41.04	63.53	<b>79.21</b>	83.40	62.72	62.67	59.85
TDA [21]	17.61	89.70	57.78	43.74	42.11	68.74	77.75	86.18	62.53	<b>64.18</b>	61.03
DPE [52]	19.80	90.83	59.26	50.18	41.67	67.60	<u>77.83</u>	85.97	64.23	61.98	61.93
CRG [51]	18.09	90.12	57.92	51.89	46.80	<b>71.09</b>	75.76	85.91	63.11	<u>63.58</u>	62.42
<b>ACE-Probability</b>	<u>21.33</u>	<u>90.91</u>	59.84	<b>55.20</b>	<b>51.02</b>	<u>70.28</u>	76.83	<b>87.95</b>	<b>65.46</b>	61.83	<b>64.07</b>
<b>ACE-Entropy</b>	<b>21.48</b>	<b>90.99</b>	<u>60.00</u>	<u>53.90</u>	<u>48.54</u>	70.08	76.91	<u>87.54</u>	<u>65.38</u>	62.60	<u>63.74</u>
CLIP-ViT-B/16	23.67	93.35	65.48	44.27	42.01	67.44	83.65	88.25	62.59	65.13	63.58
CoOp [59]	18.47	93.70	64.51	41.92	46.39	68.71	85.30	89.14	64.15	66.55	63.88
TPT [41]	24.78	94.16	66.87	47.75	42.44	68.98	84.67	87.79	65.50	68.04	65.10
DiffTPT [12]	25.60	92.49	67.01	47.00	43.13	70.10	<b>87.23</b>	88.22	65.74	62.67	65.47
TDA [21]	23.91	94.24	67.28	47.40	<u>58.00</u>	71.42	86.14	88.63	67.62	70.66	67.53
DPE [52]	28.95	94.81	67.31	54.20	55.79	75.07	<u>86.17</u>	<u>91.14</u>	70.07	70.44	69.40
CRG [51]	26.58	93.57	66.89	<u>56.38</u>	<b>59.81</b>	75.94	85.95	91.20	68.36	70.31	69.50
<b>ACE-Probability</b>	<u>29.46</u>	<u>95.13</u>	<b>68.72</b>	<u>56.38</u>	54.28	<b>77.47</b>	85.88	<b>91.47</b>	<u>70.83</u>	<u>73.62</u>	<b>70.32</b>
<b>ACE-Entropy</b>	<b>29.49</b>	<b>95.33</b>	<u>68.55</u>	<b>56.56</b>	53.63	<u>77.30</u>	85.88	<b>91.47</b>	<b>70.88</b>	<b>73.72</b>	70.28

Table 3. Performance comparisons on cross-dataset generalization across 10 fine-grained datasets. The best and second-best results are highlighted in **bold** and underlined, respectively.

ability in mitigating caching noise and enhancing classification accuracy of VLMs with increased cache capacity.

#### 4.3.2. Visualization of cache features using t-SNE

Figure 3 displays t-SNE [45] of the cached image features (with cache size  $M = 6$ ) for both DPE [57] and our method on the Food101 [2] dataset. Features from 10% of randomly selected classes are shown in different colors, while all others are indicated in gray. The visualizations demonstrate that our priority queue approach successfully gathers high-confidence samples, leading to increasingly representative visual prototypes over time.

#### 4.3.3. Efficiency Analysis

The efficiency analysis in the Table 5 shows the trade-off of different methods. Baseline zero-shot CLIP achieves 59.81% accuracy in just 9 minutes, serving as a reference for minimal overhead, while prompt-based approaches like TPT and DiffTPT deliver modest gains of +0.93% and +0.99% at significantly higher costs of 9 hours 15 minutes and 20 hours, respectively, due to backpropagation-intensive prompt optimization. Cache-based methods, including TDA (+1.54% in 1 hour 5 minutes), TPS (+1.66% in 55 minutes), and

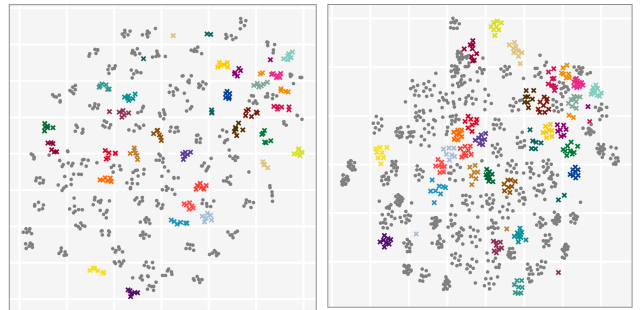


Figure 3. t-SNE [45] visualizations of the stored image features in the cache between DPE [57] and ACE-Entropy.

DPE (+3.60% in 1 hour 50 minutes), offer better efficiency through lightweight mechanisms. Notably, the proposed ACE variants stand out, with ACE-Probability attaining the highest accuracy of 64.41% (+4.60% gain) and ACE-Entropy closely following at 64.30% (+4.49% gain), both in 2 hours 40 minutes; this moderate runtime increase reflects ACE’s dynamic threshold refinement via exponential moving average and exploration updates, enabling superior robustness and generalization without prohibitive computa-

Setting	Strat.	Caltech	DTD	Flower	Pets	UCF
DPE	-	90.83	50.18	67.60	85.97	61.98
ACE w/o ZS cache	Prob.	90.55	52.54	69.51	87.41	61.81
ACE w/ ZS cache	Prob.	90.91	<b>55.20</b>	<b>70.28</b>	<b>87.95</b>	61.83
ACE w/o ZS cache	Ent.	90.39	52.19	69.39	87.00	62.18
ACE w/ ZS cache	Ent.	<b>90.99</b>	53.90	70.08	87.54	<b>62.60</b>
DPE	-	94.81	54.20	75.07	91.14	70.44
ACE w/o ZS cache	Prob.	95.06	56.21	75.80	91.21	72.06
ACE w/ ZS cache	Prob.	95.13	56.38	<b>77.47</b>	<b>91.47</b>	73.62
ACE w/o ZS cache	Ent.	95.12	56.09	74.99	91.12	72.16
ACE w/ ZS cache	Ent.	<b>95.33</b>	<b>56.56</b>	77.30	<b>91.47</b>	<b>73.72</b>

(a) Impact of zero-shot cache

Strategy	Cache size	Caltech	DTD	Flower	Pets	UCF
Prob.	M = 3	90.63	51.30	69.96	85.94	60.32
Ent.	M = 3	90.91	51.12	68.17	86.02	60.69
Prob.	M = 16	90.91	<b>55.20</b>	<b>70.28</b>	<b>87.95</b>	61.83
Ent.	M = 16	<b>90.99</b>	53.90	70.08	87.54	<b>62.60</b>
Prob.	M = 3	95.09	55.02	77.39	89.94	71.74
Ent.	M = 3	95.29	54.31	<b>77.59</b>	90.22	73.35
Prob.	M = 16	95.13	56.38	77.47	<b>91.47</b>	73.62
Ent.	M = 16	<b>95.33</b>	<b>56.56</b>	77.30	<b>91.47</b>	<b>73.72</b>

(b) Impact of cache size

Table 4. Ablation study on the impact of zero-shot cache initialization and cache size toward ACE.

Method	Testing Time	Accuracy	Gain
CLIP [38]	9 min	59.81	-
TPT [40]	9 h 15 min	60.74	+0.93
DiffTPT [11]	20 h 00 min	60.80	+0.99
TDA [22]	1 h 5 min	61.35	+1.54
TPS [44]	55 min	61.47	+1.66
DPE	1 h 50 min	63.41	+3.60
<b>ACE-Probability</b>	2 h 40 min	<b>64.41</b>	4.60
ACE-Entropy	2 h 40 min	64.30	4.49

Table 5. Efficiency analysis of ACE vs other methods.

tional demands, positioning it as a state-of-the-art solution for practical out-of-distribution adaptation.

#### 4.3.4. Cache reliability

Figure 4 visualizes the cache accuracy and overall classification performance of TDA, DPE, and our ACE across four fine-grained datasets. ACE demonstrates exceptional results, achieving an accuracy of 68.55% on Stanford Cars, surpassing TDA by 1.27% and DPE by 1.24%, and 77.30% on Oxford Flowers, outperforming TDA by 5.88% and DPE by 2.07%. These gains are complemented by ACE’s consistent superiority in cache accuracy across the datasets, reinforcing its ability in enhancing classification power while sustaining reliable and flexible decision boundaries via class-wise thresholding adaptation. The synergy between these metrics

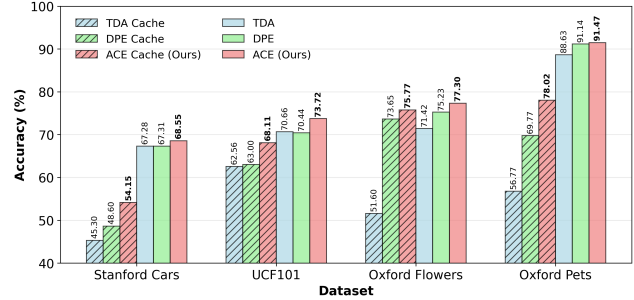


Figure 4. Comparison of cache accuracy vs. test accuracy over four datasets between TDA [21], DPE [57], and our ACE-Entropy.

underscores their complementary nature, enhancing overall performance.

#### 4.3.5. Efficiency Comparison

The inference efficiency and adaptation performance of mainstream test-time adaptation (TTA) approaches are comprehensively assessed on ImageNet [6], with the outcomes summarized in Table 5. Compared to the zero-shot CLIP [38] baseline, which achieves 59.81% top-1 accuracy within 11 minutes, ACE attains a markedly higher accuracy of 64.41% after 2 hours and 40 minutes of adaptation—representing an improvement of +4.60%. Although TPT [40] and DiffTPT [11] obtain similar accuracies of 60.74% and 60.80%, respectively, both require over 10 and 20 hours of computation, resulting in substantial computational overhead that constrains their practical applicability in efficiency-critical scenarios. TDA [22], while more efficient with a runtime of 32 minutes, achieves a lower accuracy of 61.35%. CRG [51] although achieves higher accuracy of 65.26%, it significantly requires much more time to run, result in a 3 hours running. Overall, ACE delivers the highest accuracy among all evaluated methods while maintaining a moderate adaptation time. Its adaptive components—such as dynamic curriculum thresholding and online thresholding adaptation—appears to enable faster convergence and more robust performance. These findings indicate that ACE strikes a more effective balance between adaptation speed and accuracy compared to alternative techniques, underscoring its methodological strengths in test-time adaptation.

## 5. Conclusion

In this paper, we present Adaptive Cache Enhancement (ACE), which decisively modifies class-wise thresholds to ensure the caching of more reliable test samples. Extensive benchmarking across a range of datasets and domains demonstrates that ACE outperforms state-of-the-art methods, particularly in the face of challenging distribution shifts. This approach is not merely practical; it is a robust solution for adapting vision-language models in dynamic environments. Our findings clearly show that effectively addressing noisy cache samples significantly enhances generalizability.

## References

[1] Sandhini Agarwal, Gretchen Krueger, Jack Clark, Alec Radford, Jong Wook Kim, and Miles Brundage. Evaluating clip: towards characterization of broader capabilities and downstream implications. *arXiv preprint arXiv:2108.02818*, 2021. 1

[2] Lukas Bossard, Matthieu Guillaumin, and Luc Van Gool. Food-101-mining discriminative components with random forests. In *Computer vision–ECCV 2014: 13th European conference, Zurich, Switzerland, September 6–12, 2014, proceedings, part VI 13*, pages 446–461. Springer, 2014. 6, 7, 12

[3] Mircea Cimpoi, Subhransu Maji, Iasonas Kokkinos, Sammy Mohamed, and Andrea Vedaldi. Describing textures in the wild. *2014 IEEE Conference on Computer Vision and Pattern Recognition*, pages 3606–3613, 2013. 6

[4] Mircea Cimpoi, Subhransu Maji, Iasonas Kokkinos, Sammy Mohamed, and Andrea Vedaldi. Describing textures in the wild. In *Proceedings of the IEEE/CVF Conference on Computer Vision and Pattern Recognition*, pages 3606–3613, 2014. 12

[5] Qiyuan Dai and Sibei Yang. Free on the fly: Enhancing flexibility in test-time adaptation with online em. In *Proceedings of the Computer Vision and Pattern Recognition Conference*, pages 9538–9548, 2025. 2

[6] Jia Deng, Wei Dong, Richard Socher, Li-Jia Li, Kai Li, and Li Fei-Fei. Imagenet: A large-scale hierarchical image database. In *2009 IEEE conference on computer vision and pattern recognition*, pages 248–255. Ieee, 2009. 6, 8, 12

[7] Matteo Farina, Gianni Franchi, Giovanni Iacca, Massimiliano Mancini, and Elisa Ricci. Frustratingly easy test-time adaptation of vision-language models. In *The Thirty-eighth Annual Conference on Neural Information Processing Systems*, 2024. 1, 2

[8] Li Fei-Fei, Rob Fergus, and Pietro Perona. Learning generative visual models from few training examples: An incremental bayesian approach tested on 101 object categories. In *2004 conference on computer vision and pattern recognition workshop*, pages 178–178. IEEE, 2004. 6

[9] Li Fei-Fei, Rob Fergus, and Pietro Perona. Learning generative visual models from few training examples: An incremental bayesian approach tested on 101 object categories. *Computer Vision and Image Understanding*, 106(1):59–70, 2007. 12

[10] Chun-Bei Feng, Kai Yu, Yong Liu, Salman Khan, and Wangmeng Zuo. Diverse data augmentation with diffusions for effective test-time prompt tuning. In *Proceedings of the IEEE/CVF International Conference on Computer Vision (ICCV)*, pages 2704–2714, 2023. 1, 2

[11] Chun-Bei Feng, Kai Yu, Yong Liu, Salman Khan, and Wangmeng Zuo. Diverse data augmentation with diffusions for effective test-time prompt tuning. In *Proceedings of the IEEE/CVF International Conference on Computer Vision*, pages 2704–2714, 2023. 5, 8, 14

[12] Chun-Bei Feng, Kai Yu, Yong Liu, Salman A. Khan, and Wangmeng Zuo. Diverse data augmentation with diffusions for effective test-time prompt tuning. In *2023 IEEE/CVF International Conference on Computer Vision (ICCV)*, pages 2704–2714, 2023. 6, 7

[13] Jameel Hassan, Hanan Gani, Noor Hussein, Muhammad Uzair Khattak, Muzammal Naseer, Fahad Shahbaz Khan, and Salman Khan. Align your prompts: Test-time prompting with distribution alignment for zero-shot generalization. *ArXiv*, abs/2311.01459, 2023. 1

[14] Patrick Helber, Benjamin Bischke, Andreas Dengel, and Damian Borth. Eurosat: A novel dataset and deep learning benchmark for land use and land cover classification. *IEEE Journal of Selected Topics in Applied Earth Observations and Remote Sensing*, 12(7):2217–2226, 2019. 6, 12

[15] Dan Hendrycks, Steven Basart, Norman Mu, Saurav Kadavath, Frank Wang, Evan Dorundo, Rahul Desai, Tyler Zhu, Samyak Parajuli, Mike Guo, et al. The many faces of robustness: A critical analysis of out-of-distribution generalization. In *Proceedings of the IEEE/CVF international conference on computer vision*, pages 8340–8349, 2021. 12

[16] Dan Hendrycks, Kevin Zhao, Steven Basart, Jacob Steinhardt, and Dawn Song. Natural adversarial examples. In *Proceedings of the IEEE/CVF conference on computer vision and pattern recognition*, pages 15262–15271, 2021. 6, 12

[17] Fanding Huang, Jingyan Jiang, Qinting Jiang, Hebei Li, Faisal Nadeem Khan, and Zhi Wang. Cosmic: Clique-oriented semantic multi-space integration for robust clip test-time adaptation. In *Proceedings of the Computer Vision and Pattern Recognition Conference*, pages 9772–9781, 2025. 2

[18] Ahmet Iscen, Mathilde Caron, Alireza Fathi, and Cordelia Schmid. Retrieval-enhanced contrastive vision-text models. In *The Twelfth International Conference on Learning Representations*, 2024. 1

[19] Chao Jia, Yinfai Yang, Ye Xia, Yi-Ting Chen, Zarana Parekh, Hieu Pham, Quoc Le, Yun-Hsuan Sung, Zhen Li, and Tom Duerig. Scaling up visual and vision-language representation learning with noisy text supervision. In *International Conference on Machine Learning*, pages 4904–4916, 2021. 1

[20] Jiahao Li, Yang Lu, Yuan Xie, and Yanyun Qu. Relationship prompt learning is enough for open-vocabulary semantic segmentation. In *The Thirty-eighth Annual Conference on Neural Information Processing Systems*, 2024. 1

[21] Adilbek Karmanov, Dayan Guan, Shijian Lu, Abdulmotaleb El-Saddik, and Eric P. Xing. Efficient test-time adaptation of vision-language models. In *2024 IEEE/CVF Conference on Computer Vision and Pattern Recognition (CVPR)*, pages 14162–14171, 2024. 1, 2, 3, 6, 7, 8

[22] Adilbek Karmanov, Dayan Guan, Shijian Lu, Abdulmotaleb El-Saddik, and Eric Xing. Efficient test-time adaptation of vision-language models. In *Proceedings of the IEEE/CVF Conference on Computer Vision and Pattern Recognition*, 2024. 5, 8, 14

[23] Zaid Khan and Yun Fu. Consistency and uncertainty: Identifying unreliable responses from black-box vision-language models for selective visual question answering. In *Proceedings of the IEEE/CVF Conference on Computer Vision and Pattern Recognition (CVPR)*, pages 10854–10863, 2024. 1

[24] Muhammad Uzair Khattak, Hanoona Abdul Rasheed, Muhammad Maaz, Salman H. Khan, and Fahad Shahbaz Khan. Maple: Multi-modal prompt learning. In *2023 IEEE/CVF Conference on Computer Vision and Pattern Recognition (CVPR)*, pages 19113–19122, 2022. 1

[25] Jonathan Krause, Michael Stark, Jia Deng, and Li Fei-Fei. 3d object representations for fine-grained categorization. In *Proceedings of the IEEE international conference on computer vision workshops*, pages 554–561, 2013. 6

[26] Jonathan Krause, Michael Stark, Jia Deng, and Li Fei-Fei. 3d object representations for fine-grained categorization. In *Proceedings of the IEEE/CVF International Conference on Computer Vision Workshops*, pages 554–561, 2013. 12

[27] Xiaosong Ma, Jie Zhang, Song Guo, and Wenchao Xu. Swap-prompt: Test-time prompt adaptation for vision-language models. *Advances in Neural Information Processing Systems*, 36:65252–65264, 2023. 2

[28] Subhransu Maji, Esa Rahtu, Juho Kannala, Matthew Blaschko, and Andrea Vedaldi. Fine-grained visual classification of aircraft. *arXiv preprint arXiv:1306.5151*, 2013. 6

[29] Subhransu Maji, Esa Rahtu, Juho Kannala, Matthew Blaschko, and Andrea Vedaldi. Fine-grained visual classification of aircraft. *arXiv preprint arXiv:1306.5151*, 2013. 12

[30] Sachit Menon, Ishaan Preetam Chandratreya, and Carl Vondrick. Task bias in contrastive vision-language models. *International Journal of Computer Vision*, 132(6):2026–2040, 2024. 1

[31] Maria-Elena Nilsback and Andrew Zisserman. Automated flower classification over a large number of classes. In *Indian Conference on Computer Vision, Graphics and Image Processing*, pages 722–729. IEEE, 2008. 12

[32] Maria-Elena Nilsback and Andrew Zisserman. Automated flower classification over a large number of classes. In *2008 Sixth Indian conference on computer vision, graphics & image processing*, pages 722–729. IEEE, 2008. 6

[33] Shubham Parashar, Zhiqiu Lin, Tian Liu, Xiangjue Dong, Yanan Li, Deva Ramanan, James Caverlee, and Shu Kong. The neglected tails in vision-language models. In *Proceedings of the IEEE/CVF Conference on Computer Vision and Pattern Recognition (CVPR)*, pages 12988–12997, 2024. 1

[34] Omkar M Parkhi, Andrea Vedaldi, Andrew Zisserman, and CV Jawahar. Cats and dogs. In *2012 IEEE conference on computer vision and pattern recognition*, pages 3498–3505. IEEE, 2012. 6

[35] Omkar M Parkhi, Andrea Vedaldi, Andrew Zisserman, and CV Jawahar. Cats and dogs. In *Proceedings of the IEEE/CVF Conference on Computer Vision and Pattern Recognition*, pages 3498–3505, 2012. 12

[36] Sarah Pratt, Ian Covert, Rosanne Liu, and Ali Farhadi. What does a platypus look like? generating customized prompts for zero-shot image classification. In *Proceedings of the IEEE/CVF International Conference on Computer Vision*, pages 15691–15701, 2023. 12

[37] Alec Radford, Jong Wook Kim, Chris Hallacy, Aditya Ramesh, Gabriel Goh, Sandhini Agarwal, Girish Sastry, Amanda Askell, Pamela Mishkin, Jack Clark, Gretchen Krueger, and Ilya Sutskever. Learning transferable visual models from natural language supervision. In *International Conference on Machine Learning*, 2021. 1, 2

[38] Alec Radford, Jong Wook Kim, Chris Hallacy, Aditya Ramesh, Gabriel Goh, Sandhini Agarwal, Girish Sastry, Amanda Askell, Pamela Mishkin, Jack Clark, et al. Learning transferable visual models from natural language supervision. In *International Conference on Machine Learning*, pages 8748–8763. PMLR, 2021. 5, 8, 14

[39] Benjamin Recht, Rebecca Roelofs, Ludwig Schmidt, and Vaishaal Shankar. Do imagenet classifiers generalize to imagenet? In *International conference on machine learning*, pages 5389–5400. PMLR, 2019. 6, 12

[40] Manli Shu, Weili Nie, De-An Huang, Zhiding Yu, Tom Goldstein, Anima Anandkumar, and Chaowei Xiao. Test-time prompt tuning for zero-shot generalization in vision-language models. *Advances in Neural Information Processing Systems*, 35:14274–14289, 2022. 5, 8, 14

[41] Manli Shu, Weili Nie, De-An Huang, Zhiding Yu, Tom Goldstein, Anima Anandkumar, and Chaowei Xiao. Test-time prompt tuning for zero-shot generalization in vision-language models. *ArXiv*, abs/2209.07511, 2022. 1, 2, 6, 7

[42] K Soomro. Ucf101: A dataset of 101 human actions classes from videos in the wild. *arXiv preprint arXiv:1212.0402*, 2012. 6

[43] Khurram Soomro, Amir Roshan Zamir, and Mubarak Shah. Ucf101: A dataset of 101 human actions classes from videos in the wild. *arXiv preprint arXiv:1212.0402*, 2012. 12

[44] Elaine Sui, Xiaohan Wang, and Serena Yeung-Levy. Just shift it: Test-time prototype shifting for zero-shot generalization with vision-language models. *arXiv preprint arXiv:2403.12952*, 2024. 5, 8, 14

[45] Laurens van der Maaten and Geoffrey Hinton. Visualizing data using t-sne. *Journal of Machine Learning Research*, 9: 2579–2605, 2008. 7

[46] Haohan Wang, Songwei Ge, Zachary Lipton, and Eric P Xing. Learning robust global representations by penalizing local predictive power. *Advances in Neural Information Processing Systems*, 32, 2019. 12

[47] Jianxiong Xiao, James Hays, Krista A Ehinger, Aude Oliva, and Antonio Torralba. Sun database: Large-scale scene recognition from abbey to zoo. In *2010 IEEE computer society conference on computer vision and pattern recognition*, pages 3485–3492. IEEE, 2010. 6

[48] Jianxiong Xiao, James Hays, Krista A Ehinger, Aude Oliva, and Antonio Torralba. Sun database: Large-scale scene recognition from abbey to zoo. In *Proceedings of the IEEE/CVF Conference on Computer Vision and Pattern Recognition*, pages 3485–3492, 2010. 12

[49] Chen-Wei Xie, Siyang Sun, Xiong Xiong, Yun Zheng, Deli Zhao, and Jingren Zhou. Ra-clip: Retrieval augmented contrastive language-image pre-training. In *Proceedings of the IEEE/CVF Conference on Computer Vision and Pattern Recognition (CVPR)*, pages 19265–19274, 2023. 1

[50] Tao Yu, Zhihe Lu, Xin Jin, Zhibo Chen, and Xinchao Wang. Task residual for tuning vision-language models. In *Proceed-*

*ings of the IEEE/CVF Conference on Computer Vision and Pattern Recognition*, pages 10899–10909, 2023. 2

[51] Haotian Zhai, Xinyu Chen, Can Zhang, Tianming Sha, and Ruirui Li. Mitigating cache noise in test-time adaptation for large vision-language models, 2025. 5, 6, 7, 8, 14

[52] Ce Zhang, Simon Stepputtis, Katia P. Sycara, and Yaqi Xie. Dual prototype evolving for test-time generalization of vision-language models. *ArXiv*, abs/2410.12790, 2024. 1, 2, 3, 5, 6, 7, 14

[53] Renrui Zhang, Rongyao Fang, Wei Zhang, Peng Gao, Kun-chang Li, Jifeng Dai, Yu Jiao Qiao, and Hongsheng Li. Tip-adapter: Training-free clip-adapter for better vision-language modeling. *ArXiv*, abs/2111.03930, 2021. 2

[54] Renrui Zhang, Wei Zhang, Rongyao Fang, Peng Gao, Kun-chang Li, Jifeng Dai, Yu Qiao, and Hongsheng Li. Tip-adapter: Training-free adaption of clip for few-shot classification. In *European Conference on Computer Vision*, pages 493–510. Springer, 2022. 3

[55] Taolin Zhang, Jinpeng Wang, Hang Guo, Tao Dai, Bin Chen, and Shu-Tao Xia. Boostadapter: Improving vision-language test-time adaptation via regional bootstrapping. In *The Thirty-eighth Annual Conference on Neural Information Processing Systems*, 2024. 1, 3

[56] Yabin Zhang, Wenjie Zhu, Hui Tang, Zhiyuan Ma, Kaiyang Zhou, and Lei Zhang. Dual memory networks: A versatile adaptation approach for vision-language models. In *Proceedings of the IEEE/CVF conference on CVPR*, pages 28718–28728, 2024. 1, 2

[57] Yabin Zhang, Wenjie Zhu, Hui Tang, Zhiyuan Ma, Kaiyang Zhou, and Lei Zhang. Dual memory networks: A versatile adaptation approach for vision-language models. In *Proceedings of the IEEE/CVF Conference on Computer Vision and Pattern Recognition*, pages 28718–28728, 2024. 4, 5, 6, 7, 8, 14

[58] Shuai Zhao, Xiaohan Wang, Linchao Zhu, and Yi Yang. Test-time adaptation with CLIP reward for zero-shot generalization in vision-language models. In *The Twelfth International Conference on Learning Representations*, 2024. 2

[59] Kaiyang Zhou, Jingkang Yang, Chen Change Loy, and Ziwei Liu. Learning to prompt for vision-language models. *International Journal of Computer Vision*, 130:2337 – 2348, 2021. 1, 2, 6, 7

[60] Kaiyang Zhou, Jingkang Yang, Chen Change Loy, and Ziwei Liu. Conditional prompt learning for vision-language models. In *Proceedings of the IEEE/CVF Conference on Computer Vision and Pattern Recognition (CVPR)*, pages 16816–16825, 2022. 2

[61] Kaiyang Zhou, Jingkang Yang, Chen Change Loy, and Ziwei Liu. Learning to prompt for vision-language models. *International Journal of Computer Vision*, 130(9):2337–2348, 2022. 5, 14

[62] Lihua Zhou, Mao Ye, Shuaifeng Li, Nianxin Li, Xiatian Zhu, Lei Deng, Hongbin Liu, and Zhen Lei. Bayesian test-time adaptation for vision-language models. In *Proceedings of the Computer Vision and Pattern Recognition Conference*, pages 29999–30009, 2025. 2

[63] Muzhi Zhu, Hengtao Li, Hao Chen, Chengxiang Fan, Weian Mao, Chenchen Jing, Yifan Liu, and Chunhua Shen. Seg-prompt: Boosting open-world segmentation via category-level prompt learning. In *Proceedings of the IEEE/CVF International Conference on Computer Vision (ICCV)*, pages 999–1008, 2023. 1

[64] Yuhan Zhu, Yuyang Ji, Zhiyu Zhao, Gangshan Wu, and Limin Wang. Awt: Transferring vision-language models via augmentation, weighting, and transportation. *Advances in Neural Information Processing Systems*, 37:25561–25591, 2024. 2

# Adaptive Cache Enhancement for Test-Time Adaptation of Vision-Language Models

## Supplementary Material

### 6. Appendix

In appendix, we provide additional details and experimental results to enhance understanding and insights into our proposed method. This supplementary document is organized as follows:

- **Detailed Dataset Information:** Comprehensive details about the datasets used in our experiments, including their key characteristics and distributions, are provided.
- **Textual Prompts Used in Experiments:** The text templates used in our experiments for each dataset are listed for reproducibility.
- **Full results of ablation study:** We presented further details of the ablation study on cache size and ZS cache initialization for all datasets.
- **Supplementary for different seeds:** We provide the full performance comparison of ACE for 3 different seeds on OOD experiments.

### 7. Detailed Dataset Information

In Table 6, we provide a comprehensive overview of the datasets employed in our experiments, detailing key statistics such as the number of classes, the sizes of the training, validation, and testing sets, the original tasks for which each dataset was designed. This information enables a thorough understanding of the datasets' composition and their relevance to the tasks evaluated in our study.

Dataset	Classes	Training	Validation	Testing	Task
Caltech101 [9]	100	4,128	1,649	2,465	Object recognition
DTD [4]	47	2,820	1,128	1,692	Texture recognition
EuroSAT [14]	10	13,500	5,400	8,100	Satellite image recognition
FGVCAircraft [29]	100	3,334	3,333	3,333	Fine-grained aircraft recognition
Flowers102 [31]	102	4,093	1,633	2,463	Fine-grained flowers recognition
Food101 [2]	101	50,500	20,200	30,300	Fine-grained food recognition
ImageNet [6]	1,000	1.28M	-	50,000	Object recognition
OxfordPets [35]	37	2,944	736	3,669	Fine-grained pets recognition
StanfordCars [26]	196	6,509	1,635	8,041	Fine-grained car recognition
SUN397 [48]	397	15,880	3,970	19,850	Scene recognition
UCF101 [43]	101	7,639	1,898	3,783	Action recognition
ImageNet-V2 [39]	1,000	-	-	10,000	Robustness of collocation
ImageNet-Sketch [46]	1,000	-	-	50,889	Robustness of sketch domain
ImageNet-A [16]	200	-	-	7,500	Robustness of adversarial attack
ImageNet-R [15]	200	-	-	30,000	Robustness of multi-domains

Table 6. **Detailed statistics of datasets used in experiments.** Note that the last 4 ImageNet variant datasets are designed for evaluation and only contain the test sets.

### 8. Textual Prompts Used in Experiments

In Table 7, we present a detailed compilation of the hand-crafted prompts specifically designed and utilized for each dataset in our experiments.

Dataset	Prompts
ImageNet [6]	“itap of a {CLASS}.”
ImageNet-V2 [39]	“a bad photo of the {CLASS}.”
ImageNet-Sketch [46]	“a origami {CLASS}.”
ImageNet-A [16]	“a photo of the large {CLASS}.”
ImageNet-R [15]	“a {CLASS} in a video game.”
Caltech101 [9]	“art of the {CLASS}.”
DTD [4]	“a photo of the small {CLASS}.”
EuroSAT [14]	“a photo of a {CLASS}.”
FGVCAircraft [29]	“{CLASS} texture.”
Flowers102 [31]	“a centered satellite photo of {CLASS}.”
Food101 [2]	“a photo of a {CLASS}, a type of aircraft.”
OxfordPets [35]	“a photo of a {CLASS}, a type of flower.”
StanfordCars [26]	“a photo of {CLASS}, a type of food.”
SUN397 [48]	“a photo of a {CLASS}, a type of pet.”
UCF101 [43]	“a photo of a {CLASS}, a photo of a {CLASS}.”
	“a photo of a person doing {CLASS}.”

Table 7. **Textual prompts used in experiments.** In addition to these prompts, we also employ CuPL [36] prompts to further enhance performance.

### 9. Full results of ablation study

We report full results of cross-datasets generalization settings to show the effectiveness of zero-shot statistics and choice of cache size in Table 4.

### 10. Supplementary for different seeds

We report the complete results of ImageNet with 3 different seeds in Table 9. Since we introduce the Nnever and rarely seen adaptation, and ACE is only applied during testing, the sequence of testing samples could affect the performance. Here, as we can see in Table 9, the standard deviation between datasets is stable, showing that ACE performance is not affected by randomness.

### 11. Ablation of Thresholding Components

To better understand the contribution of each part of our adaptive thresholding design, we decompose ACE into four sub-components corresponding to the individual tables in Fig. 10. Each sub-table (a)–(d) reports accuracy improvements (%) over the DPE baseline across the five datasets used in our main evaluation.

Setting	Strat.	Aircraft	Caltech	Cars	DTD	EuroSAT	Flower	Food101	Pets	SUN397	UCF101	Mean
DPE	-	19.80	90.83	59.26	50.18	41.67	67.60	77.83	85.97	64.23	61.98	61.93
w/o ZS cache	Prob.	20.97	90.55	59.63	52.54	45.94	69.51	77.47	87.41	64.92	61.81	63.08
w/ ZS cache	Prob.	21.33	90.91	59.84	55.20	51.02	70.28	76.83	87.95	65.46	61.83	64.07
w/o ZS cache	Ent.	20.37	90.39	59.37	52.19	43.89	69.39	77.48	87.00	64.99	62.18	62.74
w/ ZS cache	Ent.	21.48	90.99	60.00	53.90	48.54	70.08	76.91	87.54	65.38	62.60	63.74
DPE	-	28.95	94.81	67.31	54.20	55.79	75.07	86.17	91.14	70.07	70.44	69.40
w/o ZS cache	Prob.	29.67	95.06	68.44	56.21	55.13	75.80	86.34	91.21	70.40	72.06	70.03
w/ ZS cache	Prob.	29.46	95.13	68.72	56.38	54.28	77.47	85.88	91.47	70.83	73.62	70.32
w/o ZS cache	Ent.	30.15	95.12	68.40	56.09	54.73	74.99	86.29	91.12	70.51	72.16	69.96
w/ ZS cache	Ent.	29.49	95.33	68.55	56.56	53.63	77.30	85.88	91.47	70.88	73.72	70.28

(a) Impact of zero-shot cache												
Strat.	Cache size	Aircraft	Caltech	Cars	DTD	EuroSAT	Flower	Food101	Pets	SUN397	UCF101	Mean
Prob.	M = 3	20.34	90.63	57.27	51.30	41.02	69.96	76.41	85.94	63.72	60.32	61.69
Ent.	M = 3	19.32	90.91	57.08	51.12	42.37	68.17	76.45	86.02	63.33	60.69	61.55
Prob.	M = 16	21.33	90.91	59.84	55.20	51.02	70.28	76.83	87.95	65.46	61.83	64.07
Ent.	M = 16	21.48	90.99	60.00	53.90	48.54	70.08	76.91	87.54	65.38	62.60	63.74
Prob.	M = 3	27.69	95.09	66.26	55.02	54.14	77.39	85.50	89.94	69.38	71.74	69.22
Ent.	M = 3	28.68	95.29	66.04	54.31	53.32	77.59	85.50	90.22	69.30	73.35	69.36
Prob.	M = 16	29.46	95.13	68.72	56.38	54.28	77.47	85.88	91.47	70.83	73.62	70.32
Ent.	M = 16	29.49	95.33	68.55	56.56	53.63	77.30	85.88	91.47	70.88	73.72	70.28

(b) Impact of cache size												
Strat.	Cache size	Aircraft	Caltech	Cars	DTD	EuroSAT	Flower	Food101	Pets	SUN397	UCF101	Mean
Prob.	M = 3	20.34	90.63	57.27	51.30	41.02	69.96	76.41	85.94	63.72	60.32	61.69
Ent.	M = 3	19.32	90.91	57.08	51.12	42.37	68.17	76.45	86.02	63.33	60.69	61.55
Prob.	M = 16	21.33	90.91	59.84	55.20	51.02	70.28	76.83	87.95	65.46	61.83	64.07
Ent.	M = 16	21.48	90.99	60.00	53.90	48.54	70.08	76.91	87.54	65.38	62.60	63.74
Prob.	M = 3	27.69	95.09	66.26	55.02	54.14	77.39	85.50	89.94	69.38	71.74	69.22
Ent.	M = 3	28.68	95.29	66.04	54.31	53.32	77.59	85.50	90.22	69.30	73.35	69.36
Prob.	M = 16	29.46	95.13	68.72	56.38	54.28	77.47	85.88	91.47	70.83	73.62	70.32
Ent.	M = 16	29.49	95.33	68.55	56.56	53.63	77.30	85.88	91.47	70.88	73.72	70.28

(b) Impact of cache size

Table 8. Ablation study on the impact of zero-shot cache initialization and cache size toward ACE.

**(a) Curriculum Thresholding (CT).** Table 10a isolates the effect of CT alone. By allowing class-wise thresholds to evolve based on the model’s progress, CT already provides substantial improvements over DPE across all datasets, most notably on DTD and Flowers102. These results demonstrate that dynamically adjusting thresholds is fundamental to increasing cache purity and stabilizing early adaptation.

**(b) EMA-Based Refinement.** Adding EMA smoothing on top of CT (Table 10b) further improves accuracy on every dataset. EMA suppresses noisy fluctuations in threshold values and stabilizes pseudo-label evolution, leading to a consistent gain of roughly +1% over CT alone. This confirms that temporal smoothing is crucial for reliable threshold updates in an online setting.

**(c) Exploration for Rare Classes.** Table 10c evaluates the effect of enabling our exploration mechanism. By decreasing thresholds for underrepresented classes, exploration increases cache diversity and improves performance on datasets with high intra-class variance or long-tail structure.

The gains over (b) are the largest among all incremental components, highlighting exploration as a key driver for handling rare or difficult categories.

**(d) Zero-Shot Initialization (ZS-Init).** Finally, Table 10d shows the effect of adding zero-shot threshold initialization. ZS-Init provides a strong, distribution-aware starting point for each class, preventing early miscalibration and significantly improving early adaptation stability. When combined with CT, EMA, and exploration, ZS-Init produces the highest overall accuracy improvement, confirming its role in accelerating convergence and improving cache reliability.

**Summary.** Across all four sub-components, each contributes positively and incrementally to the final performance of ACE. The progression from (a) to (d) demonstrates that curriculum scheduling, temporal smoothing, exploration, and zero-shot initialization are individually beneficial and complementary when combined.

Method	ImageNet	ImageNet-A	ImageNet-V2	ImageNet-R	ImageNet-S	Average	OOD Average
CLIP-ResNet-50 [38]	58.16	21.83	51.41	56.15	33.37	44.18	40.69
Ensemble	59.81	23.24	52.91	60.72	35.48	46.43	43.09
CoOp [61]	63.33	23.06	55.40	56.60	34.67	46.61	42.43
TPT [40]	60.74	26.67	54.70	59.11	35.09	47.26	43.89
DiffTPT [11]	60.80	31.06	55.80	58.80	37.10	48.71	45.69
TDA [22]	61.35	30.29	55.54	62.58	38.12	49.58	46.63
TPS [44]	61.47	30.48	54.96	62.87	37.14	49.38	46.36
DMN-ZS [57]	63.87	28.57	56.12	61.44	39.84	49.97	46.49
DPE [52]	63.41	30.15	56.72	63.72	40.03	50.81	47.66
CRG [51]	<b>65.26</b>	29.69	56.07	-	-	-	-
<b>ACE-Probability</b>	<u>64.41</u> $\pm$ 0.12	<u>33.50</u> $\pm$ 0.12	<u>57.50</u> $\pm$ 0.02	<b>63.95</b> $\pm$ 0.13	<u>40.15</u> $\pm$ 0.01	<u>51.75</u> $\pm$ 0.03	<u>49.37</u> $\pm$ 0.02
<b>ACE-Entropy</b>	64.30 $\pm$ 0.12	<b>33.55</b> $\pm$ 0.12	<b>57.51</b> $\pm$ 0.03	<u>63.82</u> $\pm$ 0.15	<b>40.25</b> $\pm$ 0.02	<b>51.78</b> $\pm$ 0.04	<b>49.38</b> $\pm$ 0.01
CLIP-ViT-B/16 [38]	66.73	47.87	60.86	73.98	46.09	59.11	57.20
Ensemble	68.34	49.89	61.88	77.65	48.24	61.20	59.42
CoOp [61]	71.51	49.71	64.20	75.21	47.99	61.72	59.28
TPT [40]	68.98	54.77	63.45	77.06	47.94	62.44	60.81
DiffTPT [11]	70.30	55.68	65.10	75.00	46.80	62.28	60.52
TDA [22]	69.51	60.11	64.67	80.24	50.54	65.01	63.89
TPS [44]	70.19	60.08	64.73	80.27	49.95	65.04	63.76
DMN-ZS [57]	72.25	58.28	65.17	78.55	<b>53.20</b>	65.49	63.80
DPE [52]	71.91	59.63	65.44	80.40	52.26	65.93	64.43
CRG [51]	<b>75.01</b>	<b>63.67</b>	64.66	-	-	-	-
<b>ACE-Probability</b>	72.56 $\pm$ 0.12	<u>63.54</u> $\pm$ 0.11	<u>65.86</u> $\pm$ 0.15	<u>81.01</u> $\pm$ 0.02	52.60 $\pm$ 0.11	<u>67.05</u> $\pm$ 0.04	<u>66.01</u> $\pm$ 0.24
<b>ACE-Entropy</b>	<u>72.57</u> $\pm$ 0.14	63.47 $\pm$ 0.12	<b>65.91</b> $\pm$ 0.16	<b>81.09</b> $\pm$ 0.06	<u>52.66</u> $\pm$ 0.16	<b>67.10</b> $\pm$ 0.11	<b>66.05</b> $\pm$ 0.18

Table 9. Performance comparisons on robustness to natural distribution shifts. We present top-1 accuracy (%) results for all evaluated methods employing both ResNet-50 and ViT-B/16 visual backbones of CLIP. The best and second-best results are highlighted in **bold** and underlined, respectively.

Dataset	$\Delta$ Acc (%)	Dataset	$\Delta$ Acc (%)	Dataset	$\Delta$ Acc (%)	Dataset	$\Delta$ Acc (%)
Caltech	+0.20	Caltech	+0.30	Caltech	+0.45	Caltech	+0.32
DTD	+1.10	DTD	+1.70	DTD	+2.10	DTD	+2.18
Flowers	+0.80	Flower	+1.50	Flower	+2.30	Flower	+2.40
Pets	+0.1	Pets	+0.70	Pets	+1.50	Pets	+0.33
UCF101	+1.2	UCF	+1.40	UCF	+2.80	UCF	+3.18
<b>Average</b>	<b>+0.68</b>	<b>Average</b>	<b>+1.12</b>	<b>Average</b>	<b>+1.83</b>	<b>Average</b>	<b>+1.68</b>
(a) Effect of Curriculum Thresholding (CT) alone. Reported numbers are accuracy improvements (%) over DPE on five datasets.		(b) Effect of EMA-based refinement on top of CT. Accuracy improvements are relative to DPE.		(c) Effect of the exploration mechanism on top of CT + EMA. Accuracy improvements are relative to DPE.		(d) Impact of zero-shot initialization of class-wise thresholds added to all components. Accuracy improvements relative to DPE baseline.	

Table 10. Ablation study of each of the thresholding components.